

Expanding non homogeneous configurations of the $\lambda\phi^4$ model

Fábio L. Braghin*

Instituto de Física da Universidade de São Paulo

C.P. 66.318, C.E.P. 05315-970, São Paulo, Brasil

Abstract

A time dependent variational approach is considered to derive the equations of movement for the $\lambda\phi^4$ model. The temporal evolution of the model is performed numerically in the frame of the Gaussian approximation in a lattice of 1+1 dimensions given non homogeneous initial conditions (like bubbles) for the classical and quantum parts of the field which expands. A schematic model for the initial conditions is presented considering the model at finite fermionic density. The non zero fermionic density may lead either to the restoration of the symmetry or to an even more asymmetric phase. Both kinds of situations are considered as initial conditions and the eventual differences in early time dynamics are discussed. In the early time evolution there is strong energy exchange between the classical and quantum parts of the field as the initial configuration expands. The contribution of the quantum fluctuations is discussed especially in the strong coupling constant limit. The continuum limit is analyzed.

PACS numbers: 02.60.Nm; 03.65.Db; 07.70.+k; 05.50.+q; 11.30.Qc; 11.15.Tk; 11.90.+t.

Key-words: quantum field, condensate, hydro-dynamical expansion, non-equilibrium initial conditions, non perturbative, symmetry breaking, finite density, temperature, kink.

IFUSP- /2001.

*email:braghin@if.usp.br

1 INTRODUCTION

There are many motivations for the study of time dependent non perturbative methods in Quantum Field Theory (QFT). Some examples are immediately found in systems with strong coupling constant, spontaneously symmetry breaking and which undergo phase transitions. Some of the most interesting cases are present in the relativistic heavy ion collisions currently being prepared and performed in BNL/RHIC which probe hadronic matter at very high densities and temperatures. In these cases a region of very high energy density starts expanding (and “cooling”) just after the nuclei collision. These systems are usually described by hydro-dynamical models which are known to be quite reliable [1]. However, the understanding of these models in terms of microscopical descriptions with the underlying QFT degrees of freedom are expected to be derived and are currently being investigated by several groups. Many effects are expected to occur in those systems such as, for example, dynamical phase transitions whose existence should be present in a reliable description.

Due to the extreme complexity of realistic theories, as QCD, one usually is lead to study effective models which respect the major properties of the fundamental theory and reproduce the main issues of it in some range of a relevant variable (as energy). In the present work, however, a still more simplified version of the reality is considered in order to check qualitative effects. The $\lambda\phi^4$ model is often used as a test model, although its scalar field may be considered as the relevant degree of freedom for inflationary models in Cosmology [2]. In condensed matter and statistical mechanics it is also of interest [3]. Furthermore it can be identified to the mesonic sector of the linear sigma $O(N)$ model in the large N limit or without pions.

In the last decade a quite large amount of work have been done in order to shed light in some of the subjects mentioned above as well as aspects related to the dissipation, thermalization, decoherence, formation of disoriented chiral condensates (DCC), phase transitions among others with non perturbative time dependent formalisms. Some examples are found in [4, 5, 6, 7, 8, 9, 10], [11, 12, 13, 14, 15, 18]. Some works have already been done concerning the dynamics of non homogeneous configuration in bosonic fields. In particular, the Gaussian equations of movement were considered in [8, 9, 18] to study properties of the large time dynamics in certain cases. Non homogeneous field theory was also studied in [18] to obtain information relevant for particle production and thermalization of non-equilibrium systems.

In the present work we extend, complement and give a sounder picture for the work done in [15]. The main aspects we study in the present work are the following. Firstly a schematic model for the formation of locally non equilibrium initial conditions (which expands with time) is developed. As already proposed in this last

paper, we consider the possibility that, due to some particular condition, the condensate amplitude (as well as the physical mass of the scalars) is either suppressed or enhanced in a localized region of space. For this we consider the $\lambda\phi^4$ model coupled to fermions at finite density in a one dimensional space. Depending on the kind of the coupling the model may experience either symmetry restoration at high fermionic density or further symmetry breakdowns [16]. We look for dynamical consequences of the corresponding enhancement or suppression of the condensate at the tree level and in the frame of the Gaussian approximation. Although there are enormous differences between this simple (idealized) model (the $\lambda\phi^4$ model) and the realistic “fireballs” from RHIC, we believe that the study of the influence of the present field theoretical degrees of freedom is of interest. A partially similar idea to this one was discussed in reference [17] where the pressure due to a gas of pions, including a $\lambda\phi^4$ term in a static description, was considered to drive an expansion of a “fireball”.

We have therefore the following picture. Firstly we fix two parameters of the model, which will allow us to make meaningful comparisons between the (time dependent) tree and Gaussian levels. Secondly, it is assumed that the scalar field is locally placed in a thermal bath and/or experiences an interaction with a finite fermion density in that small region. These interactions -which change the ground state of the model- are switched off at $t=0$ yielding non equilibrium initial conditions for the scalar field which are evolved in time. The temporal evolution is performed within the tree level and Gaussian approach equations, producing the expansion of regions (bubbles) endowed with high energy densities.

The work is organized as follows. In section 2 a time dependent variational method for pure states systems is described in the Schrödinger picture and the equations of movement are derived with a Gaussian trial wave functional. Some considerations for the static and thermal case are done. The small amplitude motion case is investigated for homogeneous configurations in order to provide some useful results for analyzing the relevance of the one dimensional lattice simulations for a more realistic situation. In section 3 the numerical method using a pure states generalized density matrix - Time Dependent Hartree Bobogliubov (TDHB), as developed in [9]- is extended for the asymmetric case ($\bar{\phi} \neq 0$) in a discretized space. It allows for the investigation of the temporal evolution of a localized region of the space (lattice) where a high energy density occurs. Next, in section 4, by coupling the scalar field to a finite fermionic density system we are able to construct a model for the initial conditions at finite density. The possibility of symmetry restoration and further asymmetric phase(s) is discussed and the temporal evolution of corresponding configurations will be analysed. Still in the section 4 we provide an alternative way of fixing the parameters of the model in order to perform plausible comparisons between classical and quantum field systems. The numerical results

for the early time evolution are presented in section 5 for different initial conditions and values of the free parameters of the model. All the numerical examples shown in this article conserve total energy. Special attention is given to the strong coupling limit and one example of the temporal evolution of a deviation from a Kink solution is exhibited. The continuum limit is discussed. The results are summarized in the last section.

2 GAUSSIAN APPROXIMATION

The time dependent variational approximation at the Gaussian level has been studied for several years [5, 7, 9, 19, 20]. It provides a systematic method to study the temporal evolution of a quantum field theoretical model given an initial condition by means of the equations of movement. In spite of recent achievements for considering approximations beyond the Gaussian (for example in [11, 21]) we want to address some unexplored features in the time dependent Gaussian approach.

Let us consider the time-dependent Dirac's variational principle with a trial Gaussian wave functional [22, 23]. Firstly the average value of an action I is calculated with a given trial wave functional $|\Psi\rangle$:

$$I = \int dt \langle \Psi | (i\partial_t - H) | \Psi \rangle, \quad (1)$$

where H is the Hamiltonian.

In the Gaussian approximation at zero temperature the wavefunctional Ψ is parametrized by:

$$\Psi[\phi(\mathbf{x})] = N \exp \left\{ -\frac{1}{4} \int d\mathbf{x} d\mathbf{y} \delta\phi(\mathbf{x}) \left(G^{-1}(\mathbf{x}, \mathbf{y}) + i\Sigma(\mathbf{x}, \mathbf{y}) \right) \delta\phi(\mathbf{y}) + i \int d\vec{x} \bar{\pi}(\mathbf{x}) \delta\phi(\mathbf{x}) \right\}. \quad (2)$$

Where $\delta\phi(\mathbf{x}, t) = \phi(\mathbf{x}) - \bar{\phi}(\mathbf{x}, t)$; the normalization is N , the variational parameters are the condensate $\bar{\phi}(\mathbf{x}, t) = \langle \Psi | \phi | \Psi \rangle$ and its conjugated variable $\bar{\pi}(\mathbf{x}, t) = \langle \Psi | \pi | \Psi \rangle$; quantum fluctuations represented by the width of the Gaussian $G(\mathbf{x}, \mathbf{y}, t) = \langle \Psi | \phi(\mathbf{x}) \phi(\mathbf{y}) | \Psi \rangle$ and its conjugated variable $\Sigma(\mathbf{x}, \mathbf{y}, t)$.

The Lagrangian for a scalar field ϕ with bare mass m_0^2 and quartic coupling constant λ is given by:

$$\mathcal{L}(\mathbf{x}) = \frac{1}{2} \left\{ \partial_\mu \phi(\mathbf{x}) \partial^\mu \phi(\mathbf{x}) - m_0^2 \phi(\mathbf{x})^2 - \frac{b}{12} \phi(\mathbf{x})^4 \right\}. \quad (3)$$

From this expression the corresponding Hamiltonian H is obtained. The action of the field operator ϕ and its conjugated momentum π in functional Schroedinger representation over a wave functional $\Psi[\phi(\mathbf{x})] = \langle \phi(\mathbf{x}) | \Psi[\phi] \rangle$ is respectively:

$$\begin{aligned} \hat{\phi} |\Psi[\phi(\mathbf{x})]\rangle &= \phi(\mathbf{x}) |\Psi[\phi(\mathbf{x})]\rangle, \\ \hat{\pi} |\Psi[\phi(\mathbf{x})]\rangle &= -i\delta/\delta\phi(\mathbf{x}) |\Psi[\phi(\mathbf{x})]\rangle. \end{aligned} \quad (4)$$

The average value of the Hamiltonian, which will be explored in the numerical simulations, is given in terms of the variational parameters with the functional integrations:

$$\begin{aligned} \mathcal{H} = & \frac{1}{2} \left[\frac{1}{4} G^{-1}(\mathbf{x}, \mathbf{x}) + 4 \Sigma G \Sigma(\mathbf{x}, \mathbf{x}) + \bar{\pi}^2(\mathbf{x}) - \Delta G(\mathbf{x}, \mathbf{x}) + m_0^2 G(\mathbf{x}, \mathbf{x}) + \frac{\lambda}{4} G^2(\mathbf{x}, \mathbf{x}) + \right. \\ & \left. + m_0^2 \bar{\phi}^2 + (\nabla \bar{\phi}(\mathbf{x}))^2 + \frac{\lambda}{12} \bar{\phi}^4(\mathbf{x}) + \frac{\lambda}{2} \bar{\phi}^2(\mathbf{x}) G(\mathbf{x}, \mathbf{x}) \right]. \end{aligned} \quad (5)$$

In the Schrödinger picture the wave functional evolves like the Schroedinger equation:

$$i \frac{\partial}{\partial t} \Psi[\phi(\mathbf{x})] = H \Psi[\phi(\mathbf{x})]. \quad (6)$$

This equation is equivalent to the temporal evolution of the variational parameters given initial conditions.

The variations of the I with relation to the variational parameters (of the Gaussian wave functional) produce the equations of movement.

$$\begin{aligned} \frac{\delta I}{\delta \Sigma(\mathbf{x}, \mathbf{y}, t)} & \rightarrow \partial_t G(\mathbf{x}, \mathbf{y}, t) = 2 (G(\mathbf{x}, \mathbf{z}, t) \Sigma(\mathbf{z}, \mathbf{y}, t) + \Sigma(\mathbf{x}, \mathbf{z}, t) G(\mathbf{z}, \mathbf{y}, t)) \\ \frac{\delta I}{\delta G(\mathbf{x}, \mathbf{y}, t)} & \rightarrow \partial_t \Sigma(\mathbf{x}, \mathbf{y}, t) = \left(2 \Sigma(\mathbf{x}, \mathbf{z}, t) \Sigma(\mathbf{z}, \mathbf{y}, t) - \frac{1}{8} G^{-2}(\mathbf{x}, \mathbf{y}, t) \right) + \\ & + \left(\frac{\Gamma(\mathbf{x}, \mathbf{y}, t)}{2} + \frac{\lambda}{2} \bar{\phi}(\mathbf{x}, t)^2 \right) \\ \frac{\delta I}{\delta \bar{\pi}(\mathbf{x}, t)} & \rightarrow \partial_t \bar{\phi}(\mathbf{x}, t) = -\bar{\pi}(\mathbf{x}, t) \\ \frac{\delta I}{\delta \bar{\phi}(\mathbf{x}, t)} & \rightarrow \partial_t \bar{\pi}(\mathbf{x}, t) = \Gamma(\mathbf{x}, \mathbf{y}, t) \bar{\phi}(\mathbf{y}, t) + \frac{\lambda}{6} \bar{\phi}^2(\mathbf{x}, t) \end{aligned} \quad (7)$$

where: $\Gamma(\mathbf{x}, \mathbf{y}, t) = -\Delta + \left(m_0^2 + \frac{\lambda}{2} G(\mathbf{x}, \mathbf{x}, t) \right) \delta(\mathbf{x} - \mathbf{y})$. In the \mathbf{x} -coordinate space the Gaussian width is written as:

$$G(\mathbf{x}, \mathbf{y}) = \langle \mathbf{x} | \frac{1}{\sqrt{-\Delta + \mu^2}} | \mathbf{y} \rangle. \quad (8)$$

As it is well known the static limit of this approximation produces the “Cactus” diagrams resummation [24]. In section 3, an alternative way of writing these equations will be discussed and evolved in time in a lattice for a class of non homogeneous initial conditions. It corresponds to the time dependent Hartree Bogoliubov approximation [9].

By performing a Fourier transformation it is possible to eliminate the variables $\bar{\pi}$ and Σ . The equations in the asymmetric phase become:

$$\begin{aligned} \ddot{G}_{kk'} - \frac{\dot{G}_{kk'}^2}{2} G_{kk'}^{-1} - \frac{1}{2} G_{kk'}^{-1} + 2 \left(k^2 + m_0^2 + \frac{b}{2} G(x, x) + \frac{b}{2} \bar{\phi} \right) G_{kk'} &= 0 \\ \ddot{\phi}_k + \left(k^2 + m_0^2 + \frac{b}{6} \bar{\phi}^2 + \frac{b}{2} G(x, x) \right) \bar{\phi}_k &= 0 \end{aligned} \quad (9)$$

with $G_{\mathbf{k}\mathbf{k}'} = \langle \mathbf{k} | G(\vec{x}, \vec{x}) | \mathbf{k} + \mathbf{q} \rangle$. These equations were generalized for the out of equilibrium (non zero temperature) using different methods in [4, 10, 12, 19, 21] and they were studied extensively mainly by means

of numerical calculations. The choice of initial conditions is entirely subordinate to the approximation, in the sense that were it not Gaussian one might have to consider three conditions instead of two [23]. The analysis of these equations in show that initial conditions (for homogeneous G and $\bar{\phi}$) are crucial for the time interval in which the system evolves towards the minimum and beyond as well as for the speed of the field evolution [7, 8]. Some other effects have been addressed as, for example, dissipation via particle production, the Landau damping, collisional relaxation at zero temperature as well as the relevance of the initial conditions for the dynamics was also investigated in some cases in the early and late time evolution [6, 7, 9, 15, 25, 26, 27, 28]. In particular, it was found that the Hartree approximation is well suited for the study of early-time dynamics.

2.1 VACUUM AND RENORMALIZATION

The state of minimum energy is found from the equations of movement in the static case $\dot{G} = \Sigma = \dot{\bar{\phi}} = 0$.

The equations of motion reduce to the GAP equations which minimize the effective potential. They can then be written as:

$$\begin{aligned}\bar{\phi} \left(\frac{\lambda}{6} \bar{\phi}^2 + m_0^2 + \frac{\lambda}{2} G(\mu^2) \right) &= 0, \\ \mu^2 &= m_0^2 + \frac{\lambda}{2} \left(\bar{\phi}^2 + G(\mu^2) \right),\end{aligned}\tag{10}$$

These equations provide the two phase $\lambda\phi^4$ model: a symmetric phase (where there is only a zero condensate $\bar{\phi} = 0$) and the asymmetric phase where the condensate is non zero in the vacuum. From these equations, in the asymmetric phase, we find that:

$$\bar{\phi}^2 = \frac{3\mu^2}{\lambda},\tag{11}$$

In spite of written in terms of the bare coupling constant this value can be compared to the tree level value $\bar{\phi} = \sqrt{-\frac{6m_0^2}{\lambda}}$. In the former case (expression (11)) the bare coupling constant is fixed by the value of the renormalized coupling, as discussed below.

For a thermal environment, in d dimensions, we can perform a similar calculation to the above one with a density matrix with mixed states. It yields thermal fluctuations corrections to the two point Green's function $G(\mathbf{x}, \mathbf{x})$ which is substituted by:

$$\tilde{H}(\mu^2) = \int \frac{d\mathbf{k}}{(2\pi)^d} \langle \phi^2 \rangle_k = \int \frac{d\mathbf{k}}{(2\pi)^d} \frac{1 + \coth\left(\frac{\beta\sqrt{\mathbf{k}^2 + \mu^2}}{2}\right)}{\sqrt{\mathbf{k}^2 + \mu^2}} = \int \frac{d\mathbf{k}}{(2\pi)^d} \frac{1}{\sqrt{\mathbf{k}^2 + \mu^2}} \left(\frac{1}{2} + f(\mathbf{k}) \right).\tag{12}$$

In the above expression $f(\mathbf{k})$ is the Bose-Einstein occupation number. It is well known that these thermal fluctuations for the asymmetric phase may restore the symmetry: the vacuum solution of the condensate

$\bar{\phi}_0$ tends to become zero as temperature increases. At very high temperatures ($T \gg \mu$) the integral (12) in one spatial dimension can be expanded and the second expression of (10) can be written in one spatial dimension as:

$$\mu_T^2 = \mu^2 - \frac{\lambda}{4} \left(\frac{1}{2\beta\mu} + \frac{1}{2\pi} (\ln(\mu/(4\pi T)) + \gamma) \right) + \mathcal{O}(T^2), \quad (13)$$

where $\gamma = 0.57721$ and μ^2 is the mass at zero temperature. Therefore the physical mass is reduced at high temperatures, $\mu_T^2 = \mu^2(T) < \mu^2$. This effect is also present in the condensate (by means of expression (10)) making possible the eventual restoration of the symmetry breaking (at least at this level of approximation) [29].

The renormalization of the time dependent approach (in continuum spaces) can be done in the same way at zero and finite temperatures as well as out-of-thermodynamical equilibrium [10, 19, 20]. No additional ultraviolet divergence is found due to temporal evolution of the system or its departure from zero temperature or equilibrium. Renormalization can therefore be performed by absorbing the divergences in the physical mass (1 dimensional system) in the vacuum. By re-writing the GAP equations in terms of the renormalized quantities (m_R^2, λ_R) we can find the relationship between the bare and physical quantities. They can be written in one dimension as:

$$\begin{aligned} m_R^2(1d) &= m_0^2 + \frac{\lambda}{8\pi} \ln \left(\frac{2\Lambda}{\mu} \right), \\ \lambda_R(1d) &= \lambda \left(\frac{1 - \frac{\lambda}{8\pi m_R^2}}{1 + \frac{\lambda}{16\pi m_R^2}} \right). \end{aligned} \quad (14)$$

We note that the coupling constant acquires only a finite correction.

In a discretized space there is a natural regulator (the lattice spacing for which: $\Lambda = 1/\Delta x$). The integrals (12) become a summation and converge. As the limit to the continuum is taken the integrals tend to diverge and a redefinition of the bare quantities is needed. This will be discussed in section 5.

2.2 SMALL DEVIATIONS AROUND THE MINIMUM

Before exhibiting numerical solutions of the equation of movement in a lattice let us perform an exercise which is useful for the understanding of results. For a certain class of initial conditions it is possible to find analytical solutions for the equations of movement. Firstly because we can see the relevance of the temporal evolution of a given initial condition irrespectively to the regularization method for the local divergences. We can also check that the study of the one dimensional model can provide information about the three dimensional case.

We therefore consider the symmetric phase of the model ($\bar{\phi} = 0$) assuming a particular kind of homogeneous initial conditions (exactly the same calculation can be done for non-homogeneous asymmetric potential cases, this would not change the conclusions). Let us assume that, for some reason external to the model, the system experiences a small deviation from the state of minimum. As discussed before, this can happen because of an external thermal bath and it can be parametrized by a change in the physical mass, e.g. $m(t=0) = .9\mu$. This drives quantum fluctuations away from the ground state and generates dynamical evolution. In this case it is possible to extract exact analytical solutions for the equation of movement. For this kind of initial conditions one can linearize the Gaussian equations of motion using the following prescription for the solution:

$$G(m^2, t) = G_0(\mu^2) + \delta G(t),$$

where $G_0(\mu^2)$ is the value of the fluctuations which obey the GAP equation and $\delta G(t)$ the value of the small deviation which evolves in time.

We have presented analogue solutions for the free case in [9] choosing a plane wave prescription for the deviation $\delta G(t)$ since an infinite system is considered. We have found the following solution for the deviation $\delta G(t)$ in d-dimensions:

$$\delta G(t) = \frac{\mu^2 - m^2}{2} \frac{I_{3c}}{1 - \lambda I_3 - \frac{\lambda}{2} I_{3c}}, \quad (15)$$

where:

$$I_3 = \int \frac{d^d \mathbf{k}}{(2\pi)^d} \frac{1}{(2\sqrt{\mathbf{k}^2 + \mu^2})^3} \quad I_{3c} = \int \frac{d^d \mathbf{k}}{(2\pi)^d} \frac{\cos(2\sqrt{\mathbf{k}^2 + \mu^2}t)}{(2\sqrt{\mathbf{k}^2 + \mu^2})^3}. \quad (16)$$

The integral I_3 is time independent and contains a log divergence in 3 dimensional space. It can be absorbed in the renormalization of the mass and coupling constant. The integral I_{3c} also has a divergence at $t = 0$ in three spatial dimensions which also can be regularized. This problem was also addressed in [9, 30]. In particular, the integrals can be written in terms of generalized hypergeometric functions.

In an one dimensional space, on the other hand, there is no (ultraviolet-UV) divergences for this case of temporal evolution. Given a finite initial condition (which is the deviation from the vacuum value, proportional to $m^2 - \mu^2$) the temporal evolution is finite. This is very significant for the numerical solutions in a lattice: the temporal evolution of the system is independent of the regulator. This happens due to the fact that the static sector was separated from the dynamic evolution and the divergences only contributed for the redefinition of the former. In other words, the regularization and renormalization do not interfere in the temporal evolution. This is checked in section (5) with numerical calculations in a 1-dim lattice.

Other interesting feature can be pointed out from these solutions by rewriting them. In an 1 dimensional space the time dependent integral can be written as:

$$I_{3c}^{(1)} = \frac{(\mu^2 - m^2)}{8\pi} \int_{\mu}^{\infty} d\mathbf{y} \frac{\cos(2\mathbf{y}t)}{\mathbf{y}^2 \sqrt{\mathbf{y}^2 - \mu^2}}. \quad (17)$$

Whereas in three spatial dimensions the same time dependent integral can be written as:

$$I_{3c}^{(3)} = \frac{(\mu^2 - m^2)}{8\pi} \left(\mu^2 \int_{\mu}^{\infty} d\mathbf{y} \frac{\cos(2\mathbf{y}t)}{\mathbf{y}^2 \sqrt{\mathbf{y}^2 - \mu^2}} + \frac{\pi N_0(2\mu t)}{2} \right), \quad (18)$$

The main difference between these two expressions is the fact that in three dimensions there are two additional divergences, one of them occurs only at $t = 0$. This also suggests that the dynamics in one spatial dimension is not completely different from the dynamics in three dimensions for the cases under study.

3 NUMERICAL METHOD: Hartree Bogoliubov

This section is an extension of the work developed in [9] for the time dependent Hartree Bogoliubov approximation in the presence of a (time and space dependent) condensate. The generalized Hartree-Bogoliubov density matrix can be defined, in a discretized space, as [31]:

$$R_{i,j} = \begin{pmatrix} \rho_{i,j} & \kappa_{i,j} \\ -\kappa_{i,j}^* & -\rho_{i,j}^* \end{pmatrix}, \quad (19)$$

where the average density matrices are written in terms of the average of creation and annihilation operators: $\rho_{i,j} = \frac{1}{2} \langle a_i a_j^\dagger + a_i^\dagger a_j \rangle$ which is hermitian and $\kappa_{i,j} = - \langle a_i a_j \rangle$ is symmetric.

For the calculation of this matrix, the creation and annihilation operators are written, in a d spatial dimensions lattice, in terms of the field and its conjugate variable:

$$a(j) = \frac{1}{\sqrt{2}} \left\{ \phi(j)(\alpha)^{\frac{d-1}{2}} + i\pi(j)(\beta)^{\frac{1+d}{2}} \right\} \quad (20)$$

$$a^\dagger(j) = \frac{1}{\sqrt{2}} \left\{ \phi(j)(\alpha)^{\frac{d-1}{2}} - i\pi(j)(\beta)^{\frac{1+d}{2}} \right\}, \quad (21)$$

Where α and β are (dimensional) normalization factors. A suitable choice for them is the lattice spacing.

The averaged values of the field variables (ϕ, π) previously shown can be written in terms of the matrix elements of the above generalized matrix R . Using the notation of expressions (7,19), we obtain at zero

temperature:

$$\begin{aligned}
\langle \phi(i)\phi(j) \rangle &= G(i, j) + 1 \quad \bar{\phi}_i^2 = \frac{1}{(\Delta x)^{d-1}} \Re e(\rho(i, j) + \kappa(i, j)) \\
\langle \pi(i)\pi(j) \rangle &= F(i, j) + 1 \quad \pi_i^2 = \frac{1}{(\Delta x)^{d+1}} \Re e(\rho(i, j) - \kappa(i, j)), \\
\langle \phi(i)\pi(j) \rangle &= 2G(i, k)\Sigma(k, j) + \bar{\phi}_i\bar{\pi}_j = -2Im(\rho(i, j) - \kappa(i, j)), \\
\langle \pi(i)\phi(j) \rangle &= 2\Sigma(i, k)G(k, j) + \bar{\pi}_i\bar{\phi}_j = 2Im(\rho(i, j) + \kappa(i, j)),
\end{aligned} \tag{22}$$

where $F(i, j) = G(i, j)^{-1}/4 + 4\Sigma(i, k)G(k, l)\Sigma(l, i)$. Therefore we can already note that there are two different ways of expressing the state of the system: by means of the generalized density matrix elements OR with the variational parameters discussed before. *They are completely equivalent descriptions for the prescriptions used in this work.*

Next, we discuss the dynamics of the generalized density matrix. The temporal evolution is governed by the Hartree- Bogoliubov energy, which can be parametrized in the following form:

$$\frac{1}{2}H_{ij} \equiv \frac{\delta E}{\delta R_{ji}} = \begin{pmatrix} W_{i,j} & D_{i,j} \\ -D_{i,j} & -W_{i,j} \end{pmatrix}. \tag{23}$$

It is worth to notice that this approximation, and consequently the dynamics under study, is invariant under an unitary transformation. Therefore it is possible to consider the generalized density matrix and Hartree Bogoliubov ($H_{i,j}$) energy in another form, namely:

$$\tilde{R} = \frac{1}{\sqrt{2}}\tau R \frac{1}{\sqrt{2}}\tau^T, \quad \tilde{H} = \frac{1}{\sqrt{2}}\tau H \frac{1}{\sqrt{2}}\tau^T. \tag{24}$$

where the superscript T means the transposed matrix and τ is given by:

$$\tau = \begin{pmatrix} 1 & -1 \\ 1 & 1 \end{pmatrix}. \tag{25}$$

With these transformed matrices, one can check that a Liouville-von Neumann type equation is necessarily satisfied only in the symmetric phase ($\bar{\phi} = 0$):

$$i\dot{\tilde{R}}_{i,j} = [\tilde{H}_{i,k}, \tilde{R}_{k,j}]. \tag{26}$$

This equation can be written in terms of the averaged quantities (22). By doing this exercise we have shown that they are equivalent to equations (7) in the zero temperature limit without the condensate. When the classical field is taken into account, the equation (26) is still considered and $\bar{\phi}(x)$ acts as an external (dynamical) source to (26). The time dependence of $\bar{\phi}(t)$ is determined by the two last equations of the

set (7). These last equations, on their turn, depend on the fluctuations which are evolved in (26). We are currently extending this method to finite temperature non equilibrium systems [16]. The numerical evolution of (26) is obtained by diagonalizing $R_{i,j}$ and evolving the eigenvectors from which the variational parameters (eg. $G_{i,j}$) can be calculated.

4 PARAMETERS OF THE MODEL AND INITIAL CONDITIONS

In this section we complete the schematic model for justifying the initial conditions used in the evolution of equations of movement. The finite temperature effects were already discussed in the frame of the Gaussian approach and now we couple the $\lambda\phi^4$ model to fermions at finite density. There are many possibilities for this coupling and we discuss only a few cases which may lead either to the restoration of the spontaneously broken symmetry or to a further asymmetric model at high densities. We also provide some remarks which are helpful for the choice of the sets of parameters: physical mass μ^2 and coupling constant λ in the lattice.

4.1 $\lambda\phi^4$ COUPLED TO FERMIONS AT FINITE DENSITY

We can couple the $\lambda\phi^4$ model to fermions yielding a mechanism for placing the system in a finite fermion density environment. This procedure may produce another mechanism for the symmetry restoration. In the dynamical picture we suppose that the coupling of fermions to the scalar field is switched off at $t = 0$ as a first approximation to the problem. In part, this can be justified in the case one has decreasing scalars-fermions interaction amplitude with relation to the self interaction of the scalar field. If we consider an expanding finite density environment (“fireball”) the density is expected to decrease as the system expands. As we will not be concerned with the fermion dynamics we will only consider the interacting part of its Hamiltonian.

The following Hamiltonian density terms for spin half fermions ψ coupled to the scalar field are considered:

$$\mathcal{H}_I = g_a\phi(\mathbf{x})\bar{\psi}(\mathbf{x})\psi(\mathbf{x}) + g_b\phi^2(\mathbf{x})\bar{\psi}(\mathbf{x})\psi(\mathbf{x}), \quad (27)$$

where the coupling constants g_a and g_b are dimensionless only in 3+1 and 2+1 dimensions respectively. Nevertheless we are allowed to consider them as effective couplings of an effective theory. Eventually one would need other couplings as one considers higher energy processes.

The above couplings lead to changes in the equations of the $\lambda\phi^4$ model. In particular, we are interested in possible effects in the minimum energy state of the model. For this, we repeat the calculation of the GAP equation which is obtained by the minimization of the Hamiltonian density (expression 5) in the frame of

the Gaussian approximation. Considering that the wave functional of the system now acquires a fermionic sector $|\Xi\rangle$ (which may be a Slater determinant and is a function of the chemical potential) due to the presence of fermions at finite density we write:

$$|\Psi[\phi]\rangle \rightarrow |\Psi[\phi]\rangle \times |\Xi[\psi]\rangle. \quad (28)$$

With the fermionic wave functional one calculates the averaged values of the interacting Hamiltonian terms which enter in the effective potential of the scalar field and modify the GAP equations. These averaged terms are given in terms of a fermionic density:

$$\langle \Xi | \bar{\psi}(\mathbf{r}) \psi(\mathbf{r}) | \Xi \rangle = \rho_f(\mathbf{r}). \quad (29)$$

The density ρ_f can be calculated by fixing the chemical potential eventually at a given temperature. However it is not the aim of this work to perform such a detailed dynamical self consistent microscopic description. Here we only want to provide a physical basis for the initial conditions of the time dependent model. By the minimization of the energy density with respect to the one and two point functions of the scalar field, we obtain the GAP equations (at finite fermionic density) which can be written as:

$$\begin{aligned} \mu^2 &= m_0^2 + \frac{\lambda}{2} \left(G + \frac{\bar{\phi}^2}{2} \right) + 2g_b \rho_f, \\ \left(\mu^2 - \lambda \frac{\bar{\phi}^2}{3} \right) \bar{\phi} + g_a \rho_f &= 0. \end{aligned} \quad (30)$$

Regularization of the ultra violet divergences and the subsequent renormalization of the parameters of the model does not change qualitatively these equations.

We fix a coupling constant (a strong one: $\lambda \simeq 235\mu^2$, where μ is the physical mass) for an one dimensional system but the conclusions do not change qualitatively for higher dimensions. Solutions for these two expressions (for fixed couplings) have been searched and the main conclusions due to the introduction of the fermionic density dependence through the couplings g_a and g_b are the following:

(i) Keeping $g_b = 0$ and a quite small $g_a = +\mu/5$. As can be seen in expression (30) there will not exist the symmetric solution $\bar{\phi}_0 = 0$ at non zero density. In fact as the density increases the (real) condensate value will increase. This leads to a still more asymmetric phase.

(ii) On the other hand for the same value of the other coupling $g_b = +\mu/5$ but $g_a = 0$ the asymmetric phase will disappear when $\rho \simeq 14\mu^2$ and there will be no more condensates. At nearly double densities the physical mass also disappears.

(iii) If one assumes negative coupling $g_b < 0$ (and $g_a = 0$). In this case the condensate has increasing values for higher densities until a point where there is a complete disappearance of the asymmetric phase. This point coincides with a zero value for the mass from the GAP equation at $\rho \simeq 25\mu^2$.

For finite temperature field theories, as $O(N)$ or $O(N)XO(N)$ models. the spontaneously symmetry breakdown may be restored or not at high temperatures [32]. We point out, however, the possibility of further symmetry breaking at finite densities. A more complete analysis the finite density effects on scalar models will be shown elsewhere [16].

We obtained, therefore, another mechanism for considering local variations of the condensate: $\bar{\phi} \neq \bar{\phi}_0$. This allows for scenarios in which one obtains non homogeneous configurations for the scalar fields at finite fermionic densities and temperatures fixing the initial conditions. The situation in which the condensate is suppressed is usually more accepted. We do not neglect the possibility of enhancing the condensate due to some different phenomena when the field interact with matter.

4.2 CHOICE OF PARAMETERS

We consider static initial conditions, the initial “velocities” of the classical and quantum parts of the field are taken to be zero in all examples shown below:

$$\Sigma \propto \dot{G} = 0 \quad \pi \propto \dot{\bar{\phi}} = 0, \quad (31)$$

where the dot means time derivative.

The $\lambda\phi^4$ model has two parameters which must be fixed: mass and coupling constant. We have chosen some values to place the system in the scaling limit. With the lattice spacing $\Delta x = 0.1fm$ we had considered $\Delta x \ll \xi < L$ where $\xi = 1/\mu$ is the correlation length and L is the size of the lattice. In this region the universal properties of the lattice model can, in principle, be described by a continuum field theory. As a rule, the physical mass was chosen to be $\mu = 100MeV$ for the dynamical situations.

For the coupling constant, which has dimension fm^{-2} in one dimensional space, different values were chosen: from $\lambda = 1/12\mu^2 \simeq 0.021fm^{-2}$ to $\lambda = 600fm^{-2} \simeq 2350\mu^2$. For low dimensions the $\lambda\phi^4$ model is super-renormalizable and the coupling constant is large [33]. The smaller value was already considered to be in the non perturbative regime [11]. We have found, however, that this is not the case for the examples shown in the present work. Indeed, we have found that the dynamics for couplings with values up to $\lambda \simeq 1fm^2 \simeq 5/12\mu^2$ are not substantially different from the tree level case in the early times dynamics. Numerical examples will be shown in section 5.

In order to perform consistent comparisons between classical and quantum dynamics as well as among different initial conditions it is important to fix the parameters of the model. But instead of fixing physical mass and coupling, it is also possible to fix other variables as the energy density or particle number. For the sake of the argument, let us consider the simpler case of homogeneous solutions in the vacuum. At the tree level ($G = 0$) we obtain, in the vacuum:

$$\mathcal{H}_{vac} = -\frac{3m_0^4}{2\lambda}. \quad (32)$$

Therefore we can fix, for example, the mass and the energy density of the vacuum and calculate the corresponding coupling constant. This can be useful for the study of the influence of the quantum effects because the inclusion of fluctuations (perturbatively or not) change the ground state which is defined by the mass and coupling constant [16].

Let us consider a regularized energy density $\mathcal{H}_{G,vac}$ at the Gaussian level which can be particularly well suited for the lattice calculations. Fixing the physical mass we obtain G . Writing the total energy density with expressions (5) and (11) we obtain a second degree polynomial expression for the coupling constant. In terms of the bare (regularized) quantities the corresponding solutions for the coupling constant as a function of the (regularized) energy density are given by:

$$\lambda = \frac{-\delta \pm \sqrt{\delta^2 - 4\mu^4 G^2}}{2G^2}, \quad (33)$$

where $\delta = 8\mathcal{H}_{vac} - G^{-1} + 2\mu^2 G$. The renormalized version of \mathcal{H} (as derived, for example, in [34]) can also be used for this calculation. In one dimension there may have negative and complex solutions which do not seem to correspond to meaningful stable minima of the effective potential [16]. This calculation could be meaningful even in 3+1 dimensions to the extent that the $\lambda\phi^4$ model can be considered as effective for which the cutoff can be fixed at some high energy scale. In this case the bare and renormalized quantities can be related by expressions (14) in one spatial dimension. This is equivalent to placing the system in a lattice, which provides us with a natural cutoff ($1/\Delta x$), and to perform all calculations on it.

4.3 THE PICTURE

We have therefore the following picture. Firstly we fix two parameters of the model, which will allow us to make meaningful comparisons between the (time dependent) tree and Gaussian levels. Secondly, it is assumed that the scalar field locally experiences an interaction with a finite fermion density in a small region or has some contact with a thermal bath. These interactions -which change the ground state of the model-

are switched off at $t=0$ yielding non homogeneous (and non equilibrium) initial conditions for the scalar field which are evolved in time. The temporal evolution is performed within the tree level and Gaussian approach equations, producing the expansion of regions (bubbles) endowed with high energy densities.

4.4 INITIAL CONDITIONS: FINITE DENSITY AND TEMPERATURE

Firstly we suppose that the temperature varies continuously from the center of the lattice, where there is a high energy region, to the (zero temperature) vacuum. This constitutes an out of equilibrium situation which can be implemented in a lattice by the following configuration:

$$m^2(x, t = 0) = \mu^2 \tanh^2 \left(\frac{x - L/2}{A} \right). \quad (34)$$

The bubble of high energy density is centered at $x = L/2$ (L being the size of the lattice) and it has size given by A (which will be taken to be $0.5fm$). At the center of this bubble $m^2 = 0MeV$ which implies very high temperatures. As the temperature also modifies the order parameter of the model ($\bar{\phi}$) it may eventually yield a symmetry restoration.

We will consider another kind of configuration given by:

$$\bar{\phi}(x, t = 0) = \bar{\phi}_0 \tanh^2 \left(\frac{x - L/2}{A} \right). \quad (35)$$

In the central region of the lattice the condensate is suppressed. This can happen due to the interaction with a finite density medium. An unifying picture can be associated to the above configurations. In high energy collisions there is a large amount of energy deposited in a small region, eventually making the system to have its parameters modified, such as particle masses and condensate. This energy excess is expected to propagate (expand) in the space time.

An enhancement of the condensate due to the interaction with matter can also be assumed (it could correspond to further symmetry breaking at high densities):

$$\bar{\phi}(x, t = 0) = \bar{\phi}_0 \left[1 + \alpha \operatorname{sech}^2 \left(\frac{x - L/2}{A} \right) \right], \quad (36)$$

Where α is a real positive number which measures the amount of energy excess deposited in the central region of the lattice.

Finally, another kind of initial conditions will be considered. It corresponds to a deviation from the KINK classical solution to the equations of movement. The static KINK solution of the classical $\lambda\phi^4$ model is given by [35]:

$$\bar{\phi}(x, t = 0) = \bar{\phi}_0 \tanh \left(\frac{x - L/2}{B} \right), \quad (37)$$

where $B = \sqrt{-2/m_0^2}$. In this case $\bar{\phi}(r = 0) = -\bar{\phi}_0$ and $\bar{\phi}(r = 10) = \bar{\phi}_0$, where $r = 0$ and $r = 10$ are the borders of the lattice. This configuration can be seen as a wall which separates regions with different vacua where $\bar{\phi} = \pm\bar{\phi}_0$. It is stable at the tree level and corresponds to a non trivial topology case. By considering anti-periodic boundary conditions we have chosen a deviation with relation to the kink solution:

$$\bar{\phi}(x, t = 0) = \bar{\phi}_0 \tanh\left(\frac{x - L/2}{B}\right). \quad (38)$$

Where B was considered to be $B \simeq 1/(4\mu)$. There is an energy excess in the central region of the lattice, over the Kink.

5 NUMERICAL RESULTS

In Figure 1 some of the initial conditions for the field ($G(r)$ and $\bar{\phi}(r)$) are shown. In thick solid line it is shown $G = G(m^2(r), t = 0)$ corresponding to a bubble of high energy density which comes out from a zero mass region inside the vacuum (for $\mu = 150 MeV$). The physical mass is given by expression (34):

$$m^2(t = 0) = \mu^2 \tanh^2\left(\frac{x - L/2}{0.5}\right); \quad \bar{\phi}(t = 0) = \bar{\phi}_0.$$

In this case, it is therefore assumed that the deviation of the mass in the center of the lattice but the condensate is kept constant. The other two curves (thin solid and dotted lines) correspond to non trivial initial conditions for the condensate (35,36) and will be discussed later.

The first initial condition (34) is evolved for two different values of the coupling constant: $\lambda = \mu^2/12 \simeq 0.02 fm^{-2}$ and $600 fm^{-2}$, for a physical mass $\mu = 100 MeV$. The resulting evolution of the energy density configuration for low times are shown respectively in Figures 2 and 3. In figure 2 the energy density configuration is exhibited at different time steps: $t = 0.1 fm, 1.0 fm, 2.0 fm$ and $3.5 fm$ as a function of the lattice points. The initial (higher) energy bubble expands (by "waves") towards the extremities of the lattice distributing the initial "potential energy" over the lattice and among classical and quantum degrees of freedom. For a much stronger coupling constant, figure 3, the energy density configurations are shown and expand in a more "concentrated way" than in the weaker coupling case. Almost no difference can be seen in what concerns the expansion velocities.

The following initial condition is considered for the next cases (expression (35)):

$$\bar{\phi}(t = 0) = \bar{\phi}_0 \tanh^2\left(\frac{x - x_0}{0.5}\right), \quad \dot{\bar{\phi}} = 0.$$

In this case the condensate is suppressed in the central region of the discretized space-time. In figure 4 the evolution of the corresponding energy density is shown for a quite weak coupling constant $\lambda = 0.6 fm^{-2} \simeq 2.36\mu^2$ without quantum fluctuations, i.e., by means of the classical equation of motion -third and fourth equations of (7). Two-peak waves expand from the center of the lattice to the borders. The initial energy density has a two-peak structure which happens due to the fact that the gradient term in the Hamiltonian density has the largest values (see expression (5)). This figure can be compared to the evolution of the complete system including quantum fluctuations which is shown in figure 5. The two point function G is considered to be in the vacuum value at $t = 0$. Due to the weakness of the coupling constant (the same as the one used in figure 4) there is no visible difference between both figures. The main difference, which is quite big but not relevant to the dynamics, is the overall normalization of the energy density. The inclusion of quantum fluctuations introduces a zero point energy whose effect on the dynamics is not relevant, as the comparison between figures 4 and 5 shows. The above value of the coupling constant still is in the (dynamical) perturbative regime for this early time analysis. Comparison of this weak coupling constant case ($\lambda \simeq 1/12\mu^2$) to other works [11] suggests that the non perturbative dynamics may be present for some kind of configurations but not for others in the early time analysis.

We consider now another type of initial condition. The value of the condensate is enhanced in the central region of the lattice by means of expression (36):

$$\bar{\phi}(t=0) = \bar{\phi}_0 \left[1 + \alpha \operatorname{sech}^2 \left(\frac{x - L/2}{A} \right) \right],$$

where α is a real number which will be assumed to be in the range $0 < \alpha < 0.5$. It measures the energy of the bubble which is placed in the center of the lattice. It still has size roughly given by $A = 0.5 fm$. Since the previous examples have showed that $\lambda = 0.6 fm^{-2} \simeq 2.36\mu^2$ is not strong enough as to yield non perturbative quantum effects we consider a stronger value ($\lambda = 60 fm^{-2} \simeq 236\mu^2$) for the next figures. This configuration could correspond either to a case the model is place in a region with finite fermion density with the particular kind of coupling discussed in the previous section or to a situation where external fields would “merge” in a condensate in that small region increasing its value and the respective energy density [15].

In figure 6 the classical energy density is shown for an initial condition given above with $\alpha = 0.2$, which represents a not very energetic bubble. The energy density evolves nearly as the same way as the case of figure 4 (initial condition defined by a suppression of the condensate instead of enhancement). There is a small difference which is related to the relative amount of energy in each peak of the expanding waves

at larger times (when $t \simeq 3.5fm$). In the present case (enhancement of the condensate) the second peak is slightly higher with relation to the configuration where the condensate is suppressed (figure 4). By switching on quantum fluctuations we obtain the temporal evolution shown in figure 7. The first issue we can note is that between time steps $0.1fm$ and $1.0fm$ there is an “amplification” of the locally concentrated energy density leading regions in which its value is smaller than the vacuum energy density. These regions expand. These are local effects since the total energy is always conserved and given by the vacuum energy plus the initial bubble energy excess (positive). Furthermore, these regions tend to disappear for larger times. Another important effect is that the most part of the expanding energy is now concentrated in the “advanced” peaks, which arrive first in the extremes of the lattice. This corresponds to an acceleration of the expansion [15]. For the preceding cases the energy density “bumps” took nearly $\Delta t \simeq 5 fm$ to arrive at the borders of the lattice. In the present case (figure 7), this time is reduced to nearly $\Delta t \simeq 3.8 fm$. As noted in this last reference the energy density becomes smoother when considering the quantum fluctuations but this happens only in the non perturbative region of the coupling constant. It is also possible to note that the central region of the lattice, from where the bubble started expanding, tends to assume energy density values close to that of the vacuum as the energy goes away towards the borders of the lattice. Stronger coupling constants therefore lead to the following quantum effect: there is an acceleration of the energy density expansion. Although the two-peaked form of the expanding waves persists, the advanced peaks (those which arrive before to the borders of the lattice) are strengthened with relation to the others. This is a clear indication that the expansion is faster corresponding to a non perturbative quantum effect.

What happen if the initial energy density excess in the center of the lattice is increased? In figures 8 and 9 this is shown respectively for the classical system and for the “complete” (classical plus quantum) field with the same set of parameters as the preceding figures but considering $\alpha = 0.5$ in expression (36). The coupling constant is in the range $\lambda = 60fm^{-2} \simeq 236\mu^2$. The energy density excess is much higher than those considered before as it can be checked by comparing with figure 8. In this figure the temporal evolution of the energy density of the condensate without quantum fluctuations is shown. In spite of different normalization and energy values the classical dynamics is not modified with relation to figure 4 (for which the initial condition was given by the suppression of the condensate with expression (35)). In figure 9 the dynamics of quantum fluctuations is taken into account. It is also noted in this case a quite large energy density amplification in the beginning of the evolution and the existence of expanding regions in which the energy density is smaller than the value of the vacuum. They modify the two-peak structure discussed before. Although the last step in such time evolution present values for the energy density which may not

be completely reliable due to numerical uncertainties the main issues are completely trustful even because, we emphasize, the total energy is conserved. The acceleration found before still is present. Moreover, it is interesting to note that there is little difference between the temporal evolution of cases in which initial conditions are given in term of α with different values, i.e., for $\alpha = 0.2$ or $\alpha = 0.5$ in the early time dynamics.

For the examples shown above only the short time behavior was analyzed. These are so short time scales that the boundary conditions are not even relevant. The large time behavior was briefly studied for some cases in the strong coupling limit ($\lambda = 60 fm^{-2}$). No equilibration was found for larger times evolutions, i.e., the amplitude of the (classical and quantum) oscillations do not tend to zero. There are several other different approaches dealing with different aspects of the non-equilibrium field dynamics [13, 18, 21, 36].

In the next figures another kind of (non trivial) initial configuration is considered for the condensate. In this case $\bar{\phi}(r = 0) = -\bar{\phi}_0$ and $\bar{\phi}(r = 10) = \bar{\phi}_0$, where 0 and 10 are the borders of the lattice. This configuration can be seen as a wall which separates regions with different vacua where $\bar{\phi} = \pm\bar{\phi}_0$. By considering anti-periodic boundary conditions we have chosen a deviation with relation to the KINK solution (expression 38) [35]:

$$\bar{\phi}(x, t = 0) = \bar{\phi}_0 \tanh\left(\frac{x - L/2}{B}\right). \quad (39)$$

Where B was considered to be $B \simeq 1/(4\mu)$ and $\lambda = 60 fm^{-2}$. Firstly the evolution of the equations of movement for the condensate without quantum fluctuations ($G = 0$) is performed. In figure 10a the resulting classical field profile ($\bar{\phi}(t)$) at the points $x = 5 fm$ and $x = 10 fm$ are shown. The change of the field at $\bar{\phi}(x = 10, t)$ (there is a “flip”) is due to the anti-periodic boundary conditions and happens exactly at the time when the energy density bumps arrive at the border of the lattice. The field in the central region has a static and constant value given at $t = 0$. In figure 10b we show the energy density expansion (it does not have the two-peak structure due to the initial condition). By switching on quantum fluctuations we obtain figures 11a, b, c. In figure 11a the condensate in the same points of the lattice as in figure 10a is shown. The dynamics is similar but the field (at $r=10 fm$) “flips” to the other vacuum value faster. In figure 11b the deviation of the quantum fluctuations with relation to the value in the vacuum, at the same points ($\delta G(t, r) = G(t, r) - G_0$), are shown. They clearly exhibit the energy transfer between classical and quantum degrees of freedom. In particular, when the “condensate flip” occurs, the quantum fluctuations are enhanced in the corresponding point ($r = 10 fm$). For the energy density configurations, in figure 11c, there is no strong effect with relation to the purely classical dynamics (seen in figure 10b).

For the figures 12 and 13 a different size of the bubble of suppressed condensate is considered with

the initial condition given by expression (35). We have considered half value, i.e., $A = 0.25fm$. This yields a smaller region out of equilibrium. In figure 12 the temporal evolution of the energy density of the classical condensate case is shown as well as in figure 13 the same for the classical plus quantum system. The concentration of energy density in the “advanced” peaks discussed before (figures 5,7 and [15]) is well visible in figure 13. This indicates, again, an acceleration of the expansion with relation to the classical dynamics. Moreover, there is the appearance of new bumps in the expansion due to the inclusion of the quantum dynamics in a finite (discrete) system.

In the continuum limit the GAP equations and the equations of movement present the ultraviolet (UV) divergences discussed in section 2. This is reproduced in the lattice calculations and to show that our results do reproduce features of the continuum renormalized model we have studied the limit of smaller lattice spacings down to $\Delta x = 0.02fm$. In order to continue in the scaling limit the mass μ^2 must be changed in the same way as the GAP equations in the lattice since it absorbs the UV infinities in the renormalization. The two point function scales as [33]:

$$G^{-1} \rightarrow \frac{2\kappa}{(\Delta x)^2 Z_R} \left(m_R^2 + p^2 + o(p^4) \right), \quad (40)$$

where Z_R is the field renormalization factor (it is finite in the 1+1 dimensional case). Results for the small lattice spacing limit are not visibly modified. The difference is found in the normalizations (absolute values) of the two point function and of the energy density. By subtracting these values by the vacuum ones the results remain unchanged. Besides that, the dynamics is not affected by these divergences, i.e., by the regularization method. This was shown in section 2.3 for the particular case of initial conditions given by small deviations from the vacuum.

6 SUMMARY

We have analyzed the temporal evolution of expanding non-homogeneous configurations of the $\lambda\phi^4$ model considering two different approaches: the classical equations of motion and compared its results to the equations of motion in the frame of the Gaussian variational approximation in a 1+1 dimensional lattice. A schematic model for the model at finite fermionic density has been drawn for the initial conditions and the equations of movement have been solved. The condensate may either disappear (symmetry restoration) or become higher (no symmetric phase, with further symmetry breaking) at higher densities. The parameters of the $\lambda\phi^4$ model were fixed in order to allow a comparison between the classical and quantum field temporal

evolution. We have been able to study the influence of the quantum fluctuations on the classical field dynamics for different sets of free parameters. By varying the parameters of the model and the non-homogeneous initial conditions we have carefully investigated the expansion of different field configurations in the frame of the Gaussian approximation. The quantum fluctuations accelerate the expansion of a concentrated configuration of the field. This effect is considerable for strong coupling constants and particular cases of the initial conditions, namely when there is an enhancement of the condensate (stronger symmetry breaking) instead of suppression (restoration). However, no big differences were found for these two different initial conditions in the early time dynamics. Closely related works have been done by [8, 11, 27] respectively for other initial conditions, as for instance a Gaussian configuration, and additional averaging over ensembles of mean fields (which seems to lead to thermalization at long times). It is possible to conclude that the initial conditions play an important role in the temporal evolution. We have been concerned mainly with short time intervals evolution and other issues related to thermalization and equilibration have not been addressed extensively.

Acknowledgements

This work was supported by FAPESP- Brazil. F.L.B. wishes to thank F.S. Navarra for several interesting discussions and a collaboration. The numerical calculations were performed in the machines of the Laboratory for Computation of the University of São Paulo - LCCA-USP.

References

- [1] U. Heinz, hep-ph/9902424; F.Grassi, Y. Hama and T. Kodama, Z. Phys. **C 73** 153, (1996); and references therein.
- [2] D.H. Lyth, A. Riotto, Phys. Rept.**314**, 1 (1999).
- [3] A.J. Heeger, S. Kivelson, J.R. Schrieffer, W.P. Su, Rev. Mod. Phys. **60**, 781 (1988); G. Grüner, Rev. Mod. Phys. **60**, 1129 (1988).
- [4] O. Éboli, R. Jackiw and So Young Pi, Phys. Rev. **D37**, 3557 (1988).
- [5] F. Cooper, S.-Y. Pi and P.N. Stancioff, Phys. Rev. **D 34**, 3831 (1986).
- [6] F. Cooper, S. Habib, Y. Kluger, E. Mottola, Phys. Rev. **D 55**, 6471 (1997).

- [7] D. Boyanovsky, M.D'Attanasio, H. J. de Vega, R. Holman, D.-S. Lee, Phys. Rev. **D 52**, 6805 (1996);
D. Boyanovsky, H. de Vega, R. Holman, D.S. Lee, A. Singh, Phys. Rev. **D 51**, 4419 (1995).
- [8] D. Boyanovsky, H.J. de Vega, R. Holman, Phys. Rev. **D 51**, 734 (1995); Phys. Rev. **D 54**, 1748 (1996);
D. Boyanovsky, F. Cooper, H.J. de Vega, P. Sodano, hep-ph/9802277.
- [9] F.L. Braghin, Phys. Rev. **D 57**, 3548, (1998).
- [10] J. Baacke, K. Heitmann, C. Pätzold, Phys. Rev. **D 57**, 6406 (1998); J. Baacke, K. Heitmann, C.
Pätzold, Phys. Rev. **D 57** 6406, (1999); J. Baacke and K. Heitmann, hep-ph/0003317.
- [11] M. Sallé, Jan Smit and J. C. Vink, hep-ph/0012362; hep-ph/0012346.
- [12] A. Berera, M. Gleiser, R.O. Ramos, Phys. Rev. **D 58**, 123508-1 (1998).
- [13] G. Aarts, G.F. Bonini, C. Wetterich, hep-ph/0003262; hep-ph/0007357; G. Aarts and J. Berges,
hep/0103049; J. Berges, hep-ph/0105311.
- [14] Y. Tsue, A. Koike, N. Ikezi, hep-ph/0103246.
- [15] F.L. Braghin and F.S. Navarra, Phys. Lett. **B 508**, 243 (2001).
- [16] F.L. Braghin, *in preparation*.
- [17] A. Dumitru et al., nucl-th/0010107.
- [18] G. Aarts and J. Smit, hep-ph/9906538.
- [19] F. Cooper, S. Habib, Y. Kluger, E. Mottola, J.P. Paz and P.R. Anderson, Phys. Rev. **D50**, 2848 (1994).
- [20] Pi, S.Y. , M. Samiullah, Phys. Rev. **D 36**, 3128 (1987).
- [21] J. Berges, J. Cox, hep-ph/0006160.
- [22] R. Jackiw and A. K. Kerman, Phys. Lett **A71**, 158 (1979).
- [23] F. Cooper and E. Mottola, Phys. Rev. **D36**, 3114 (1987).
- [24] T. Barnes and G.I. Ghandour, Phys. Rev. **D22**, 924 (1980).
- [25] P.L. Natti, A.F.R. de Toledo Piza, Phys. Rev. **D 54**, 7867 (1996).

- [26] G. Aarts, G.F. Bonini and C. Wetterich, hep-ph/0007357.
- [27] L.M.A. Bettencourt, K. Pao, J.G. Sanderson, hep-ph/0104210
- [28] C. Destri, E. Manfredini, hep-ph/0001177; hep-ph/0001178.
- [29] L. Dolan and R. Jackiw, Phys. Rev. **D 9**, 3321 (1974); G. Bimonte, D. Iniguez, A. Tarancon, C.L. Ullod, Nucl. Phys. **B 515**, 345 (1998).
- [30] J. Baacke, D. Boyanovsky, H. de Vega, hep-ph/9907337.
- [31] J.P. Blaizot and G. Ripka, *Quantum Theory of Finite Systems*, The MIT Press, Cambridge, (1986).
- [32] S. Weinberg, Phys. Rev. **D 9**, 3357 (1974); M.B. Pinto, R.O. Ramos, Phys. Rev. **D 61**, 125016 (2000).
- [33] J. Zinn Justin, *Quantum Field Theory and Critical Phenomena*, 3rd edition, Oxford University Press, Oxford (1996).
- [34] P.M. Stevenson, Phys. Rev. **D 32**, 1389 (1985). A.K. Kerman, C. Martin, D. Vautherin, Phys. Rev. **D 47**, 632 (1993).
- [35] I. Montvay and G. Münster, *Quantum Fields on a Lattice*, Cambridge Univ. Press, Cambridge (1984).
- [36] Sz. Borsányi, Zs. Szép, hep-ph/0011283; A. Jakovác, A. Patkós, P. Petreczky, Zs. Szép, Phys. Rev. **D 61**: 025006 (2000).

Figure Captions

Fig. 1 Examples of initial field configuration. Thick solid line corresponds to the two point function $G(r, t = 0)$ for the initial condition (34) considering $\mu = 150 MeV$. Thin solid and dotted lines correspond to the initial condensate configuration of expressions (35) and (36 with $\alpha = 0.2$) respectively.

Fig. 2 Evolution of the energy density of the field (classical + quantum) at different times. The initial time mass configuration is given by (34) and $\lambda = \mu^2/12$.

Fig. 3 The same as Fig.2 with $\lambda = 600 fm^{-2}$.

Fig. 4 Evolution of the energy distribution of the classical field for the initial configuration (35) and $\lambda = 0.6 fm^{-2}$.

Fig. 5 Evolution of the energy distribution of the field with the quantum fluctuations for initial configuration (35) and $\lambda = 0.6fm^{-2}$.

Fig. 6 Evolution of the energy distribution of the classical field for the initial configuration (36) with $\alpha = 0.2$ and for $\lambda = 60fm^{-2}$.

Fig. 7 Evolution of the energy distribution of the field with the quantum fluctuations for initial configuration (36) with $\alpha = 0.2$ and $\lambda = 60fm^{-2}$.

Fig. 8 Evolution of the energy distribution of the classical field for the initial configuration (36) $\alpha = 0.5$.

Fig. 9 Evolution of the energy distribution of the field with the quantum fluctuations for initial configuration (36) with $\alpha = 0.5$ and $\lambda = 60fm^{-2}$.

Fig. 10 Evolution of the energy distribution of the classical field $\bar{\phi}(t, x)$ for the initial configuration (37) and $\lambda = 60fm^{-2}$.

Fig. 11 Evolution of the energy distribution of the field with the quantum fluctuations for initial configuration (37) with $\lambda = 60fm^{-2}$.

Fig. 12 Evolution of the energy distribution of the classical field for the initial configuration (35) with $A = 0.25fm$.

Fig. 13 Evolution of the energy distribution of the field with the quantum fluctuations for initial configuration (35) with $A = 0.25fm$.

Figure 1

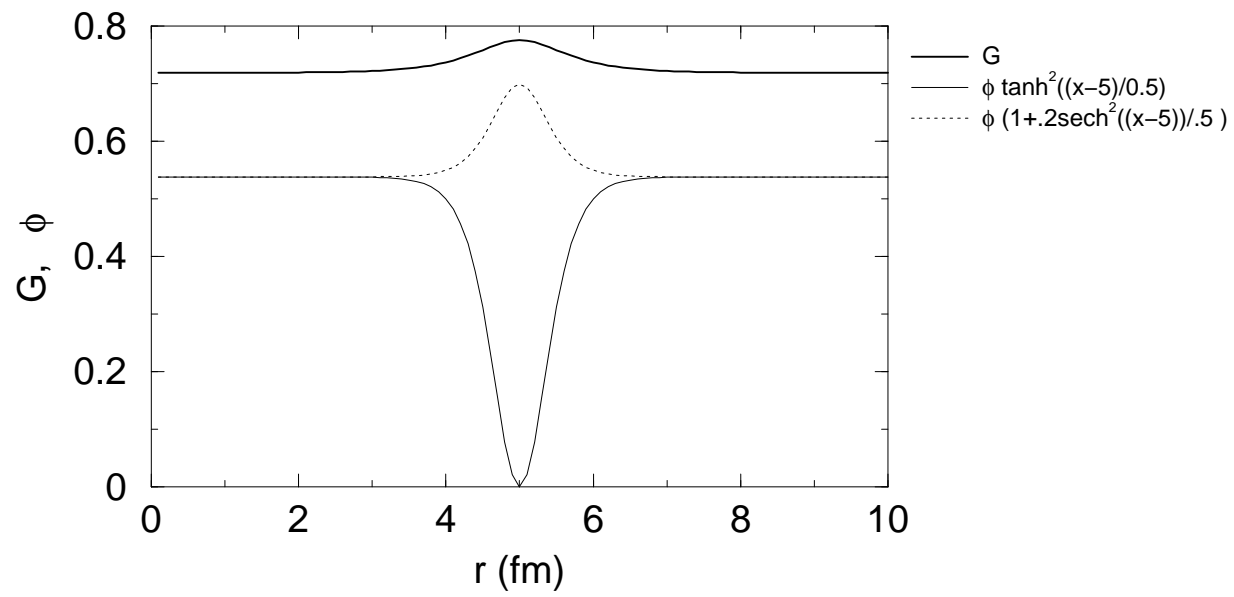


Figure 2

$$\lambda = m/12$$

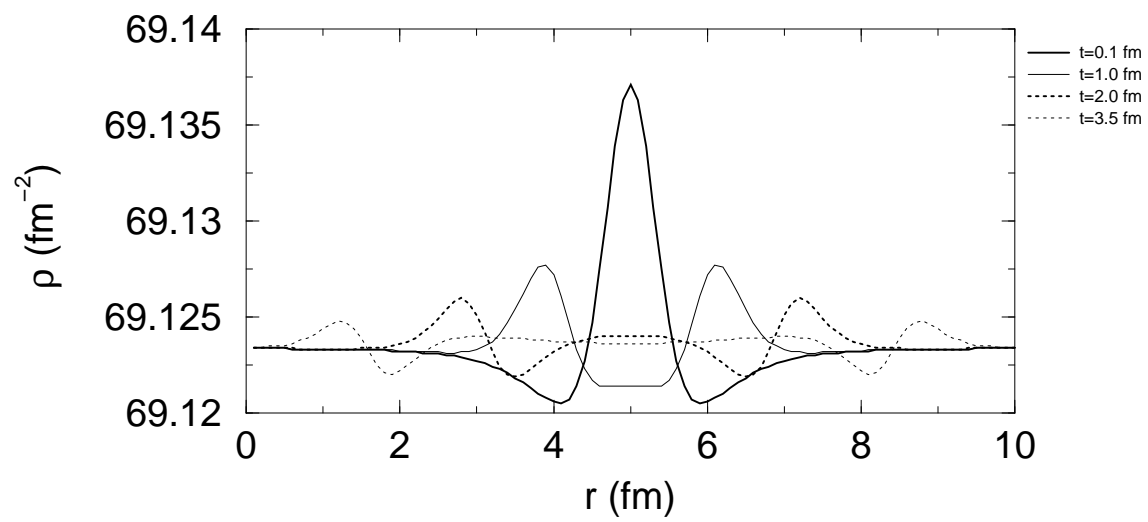


Figure 3

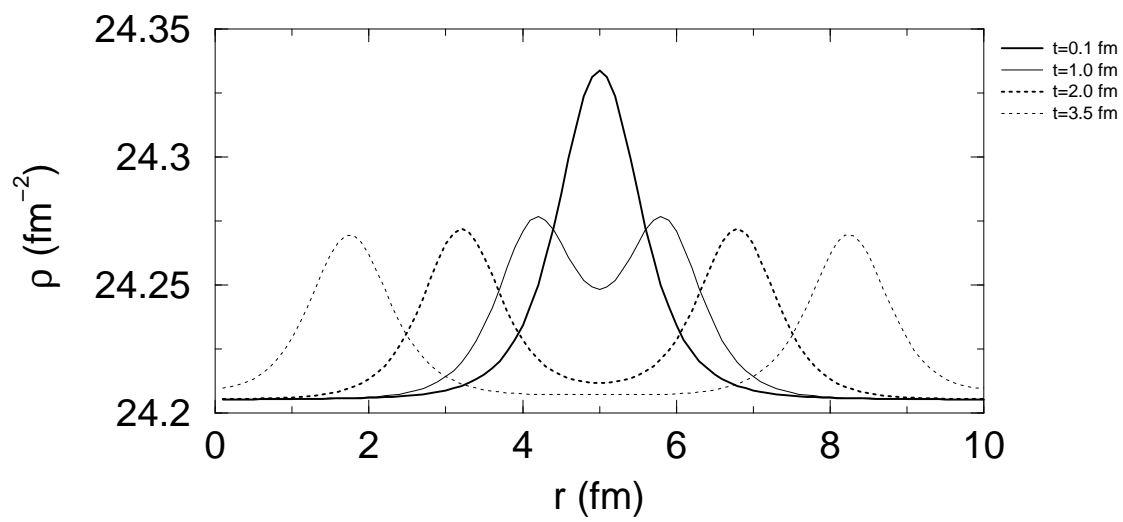


Figure 4

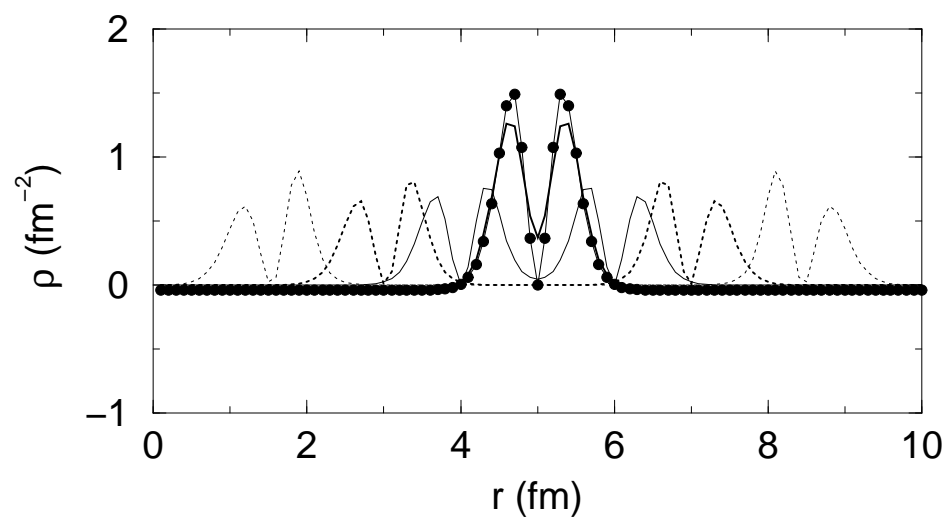


Figure 5

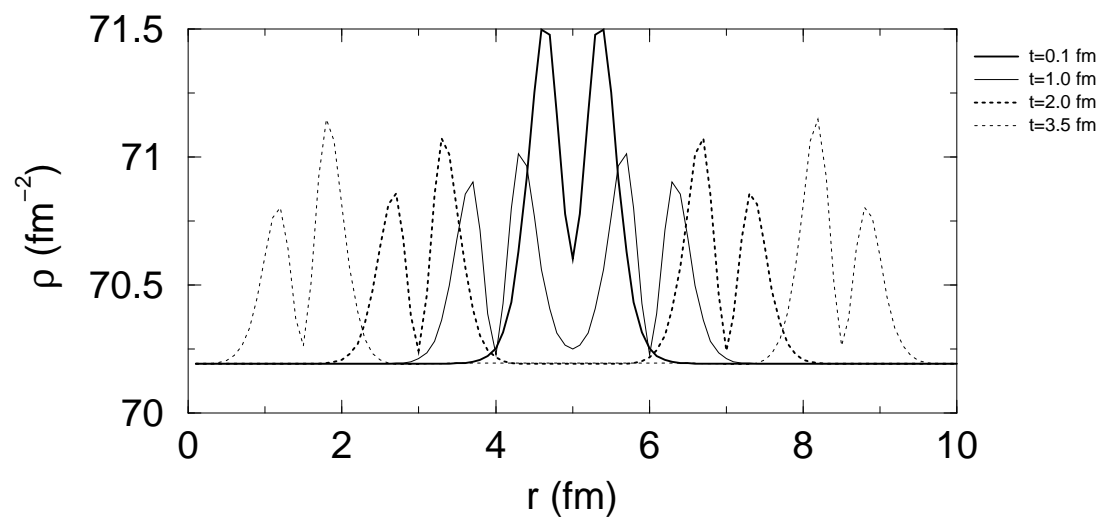


Figure 6

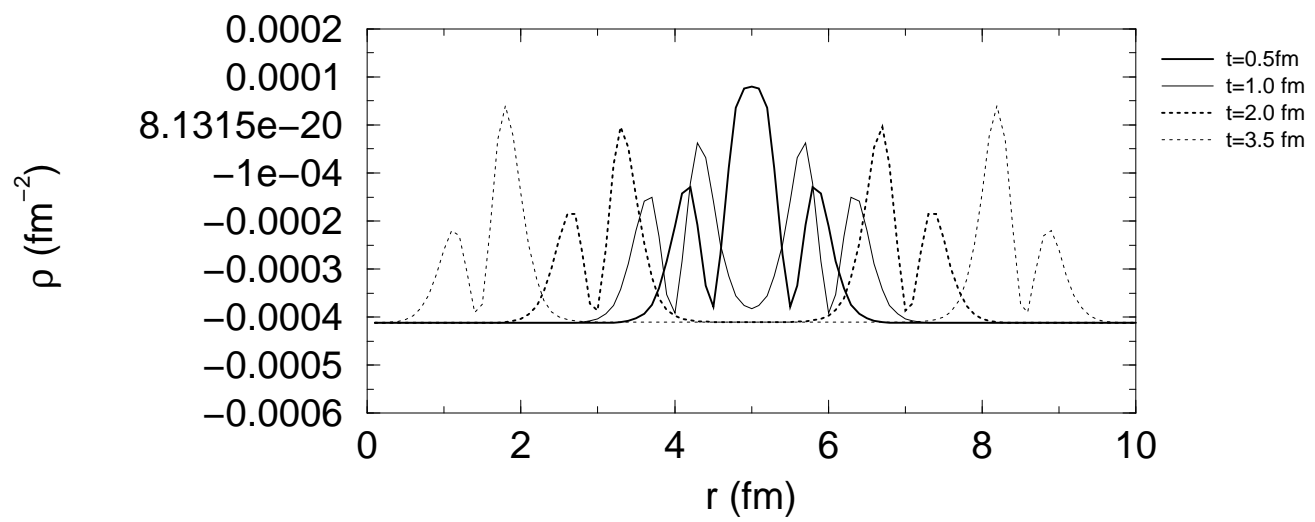


Figure 7

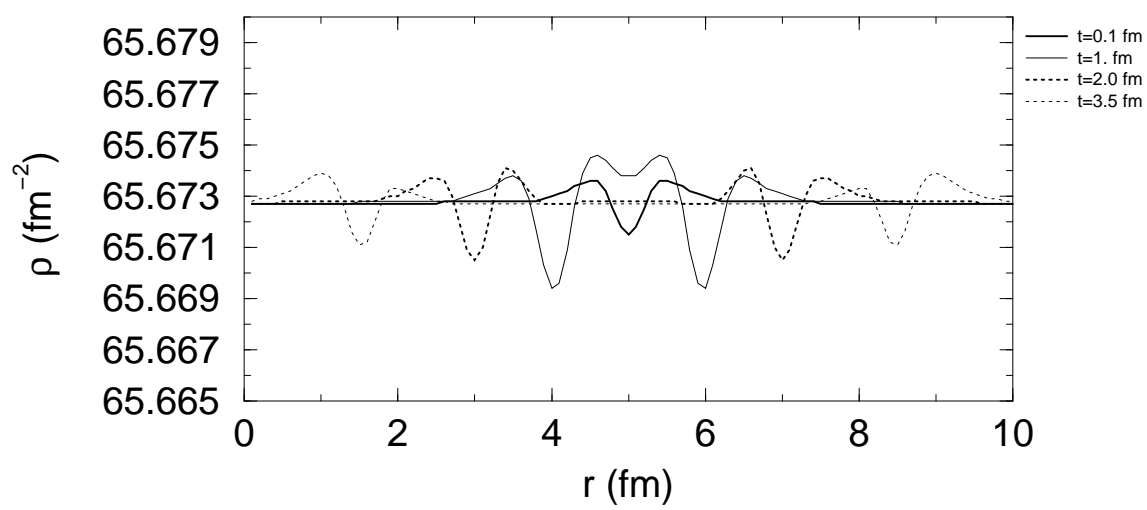


Figure 8

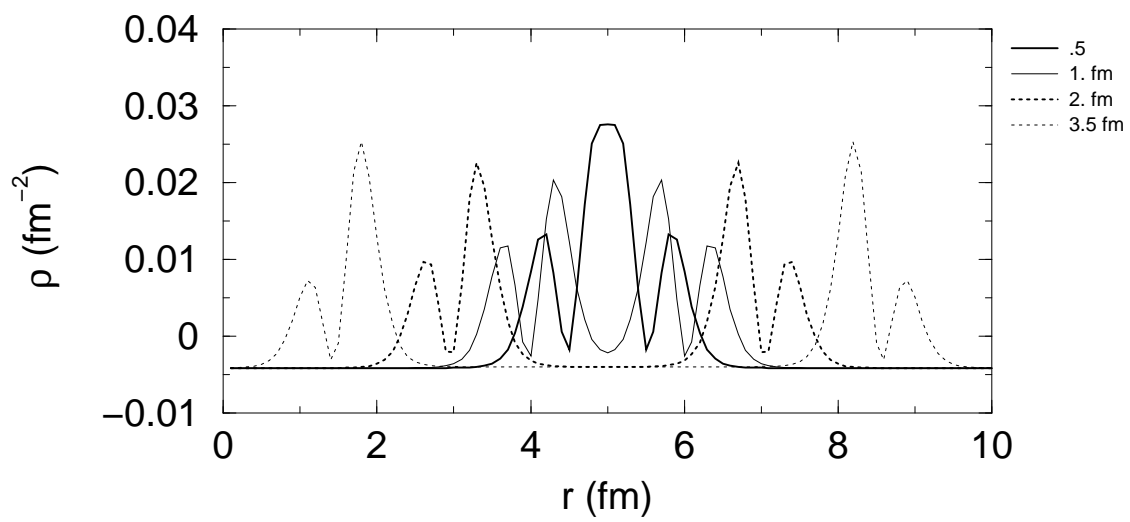


Figure 9

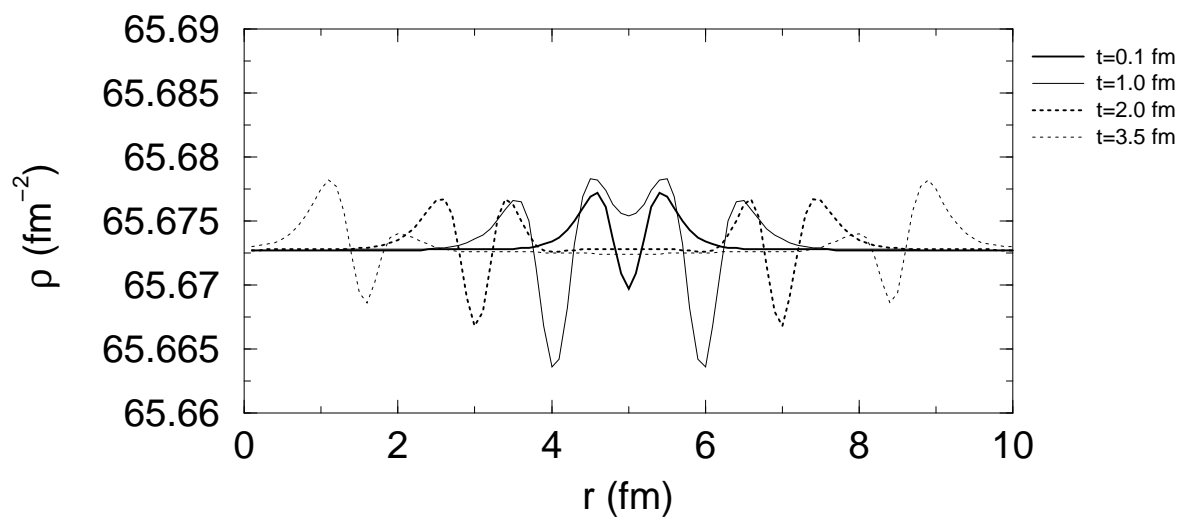


Figure 10a

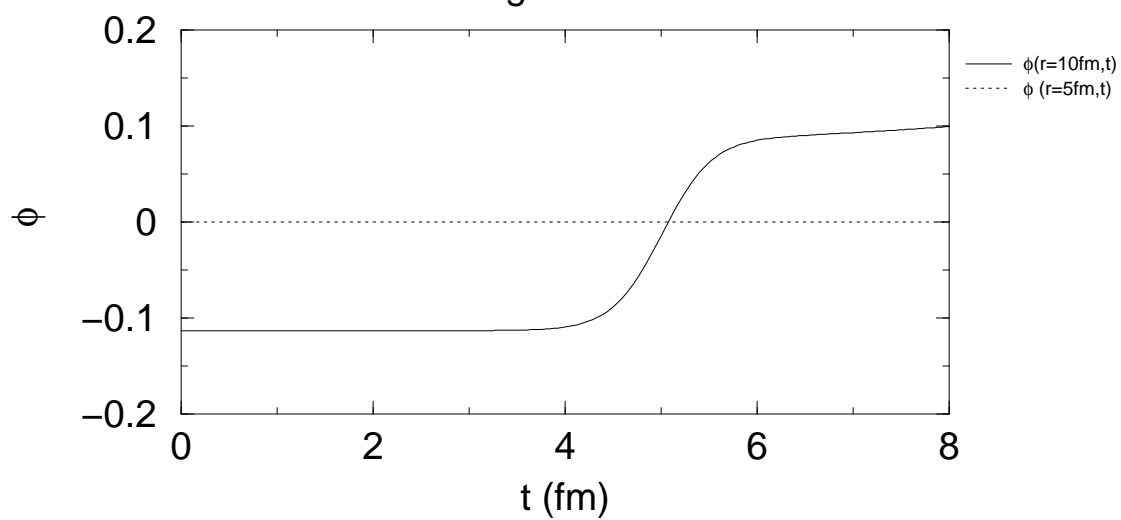


Figure 10b

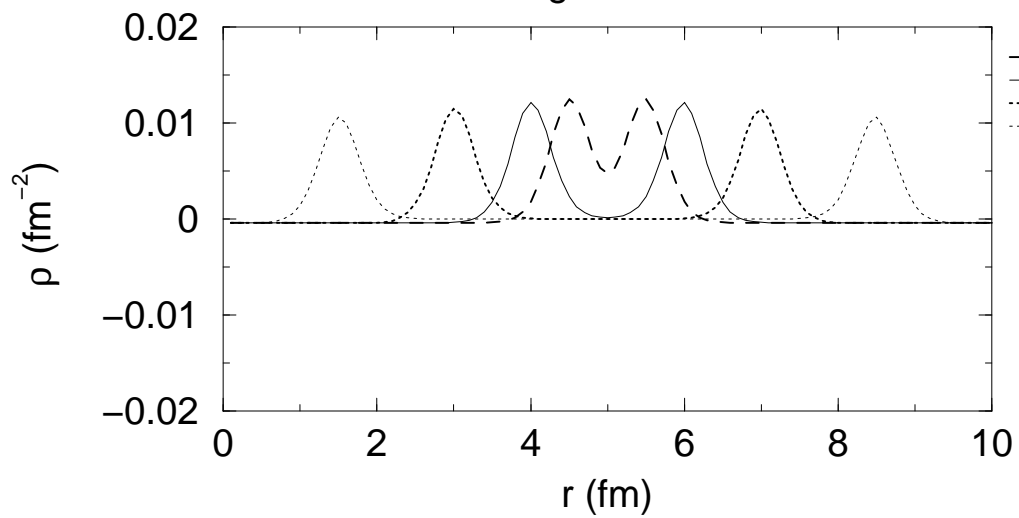


Figure 11a

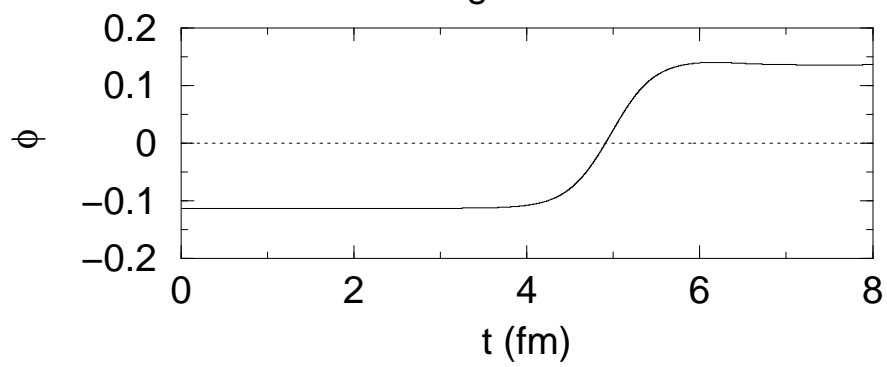


Figure 11b

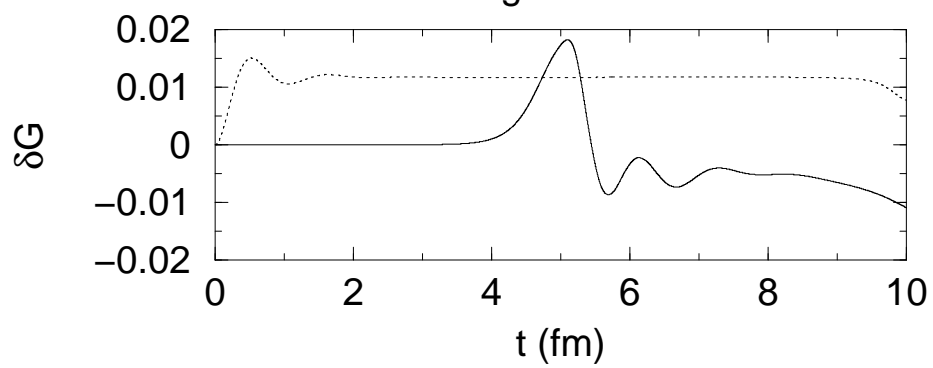


Figure 11c

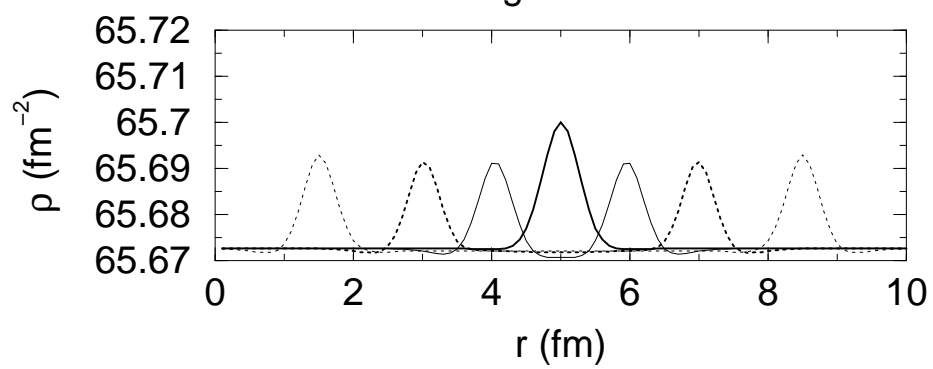


Figure 12

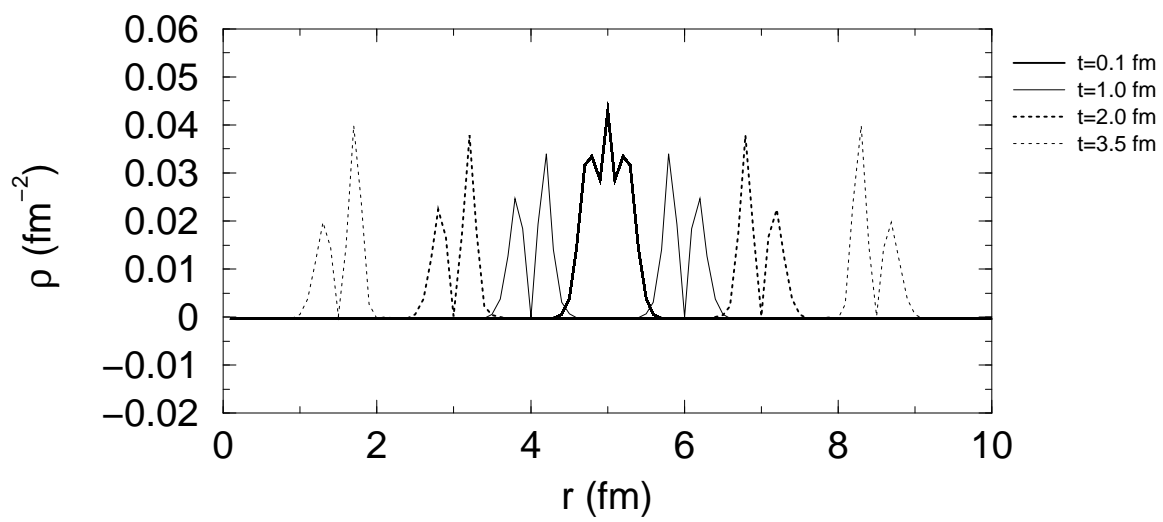


Figure 13

